

Supporting Information

A Tumor Treatment Strategy Based on Biodegradable BSA@ZIF-8 for Simultaneous Ablating Tumor and Inhibiting Infection

Qiong Wu^a, Mei Li^d, Longfei Tan^a, Jie Yu^b, Zengzhen Chen^a, Lihui Su^a, Xiangling Ren^a, Changhui Fu^a, Jun Ren^a, Laifeng Li^a, Feng Cao^c, Ping Liang^b, Yu Zhang^d, and Xianwei Meng^{a,*}

^a Laboratory of Controllable Preparation and Application of Nanomaterials, Key Laboratory of Cryogenics, Technical Institute of Physics and Chemistry, Chinese Academy of Sciences, No.29 East Road Zhongguancun, Beijing 100190, P. R. China

E-mail: mengxw@mail.ipc.ac.cn

^b Department of Interventional Ultrasound, Chinese PLA General Hospital, Beijing 100853, P. R. China

^c Department of Cardiology, Chinese PLA General Hospital, Beijing 100853, P. R. China

^d Department of Orthopedics, Guangdong Key Lab of Orthopedic Technology and Implant, Guangzhou General Hospital of Guangzhou Military Command, Guangzhou, Guangdong 510010, P. R. China

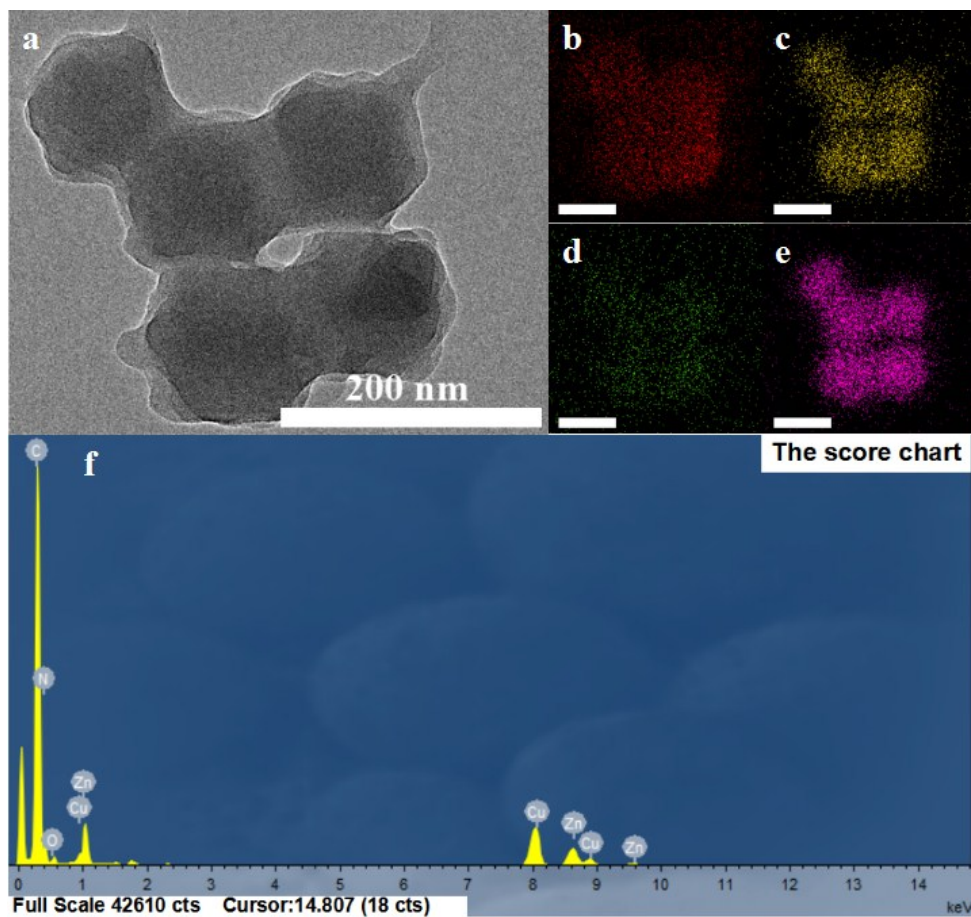


Figure S1. (a) TEM image of BSA@ZIF-8. (b-e) Element mapping for b) carbon, c) nitrogen, d) oxygen, and e) zinc, scale bar is 100 nm. (f) TEM EDS of BSA@ZIF-8.

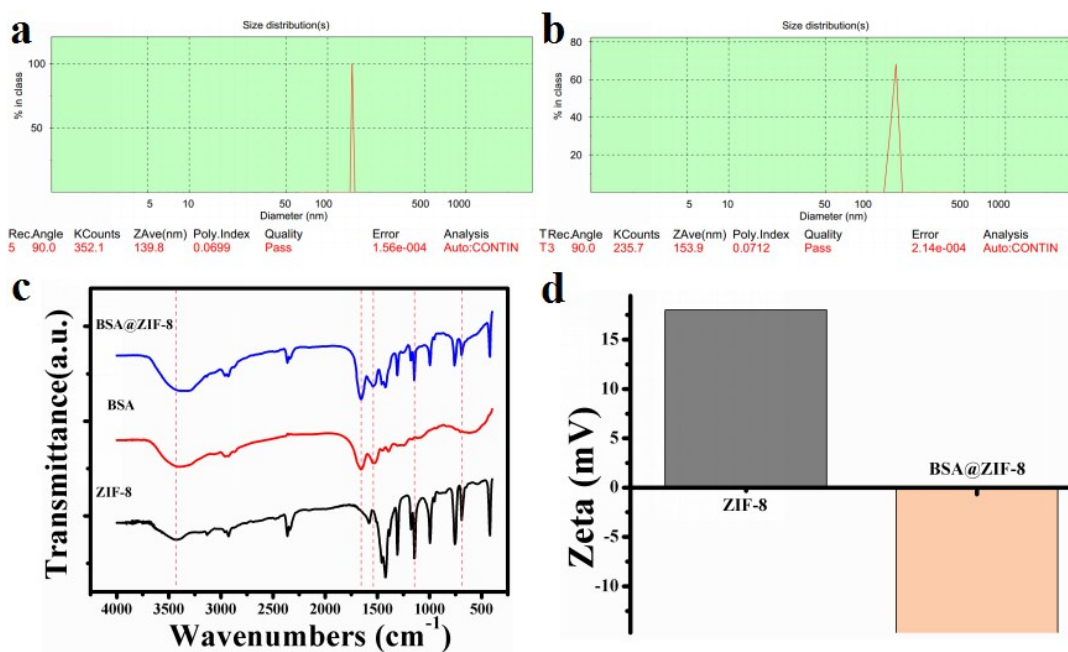


Figure S2. (a) Hydrodynamic size of ZIF-8. (b) Hydrodynamic size of BSA@ZIF-8. (c) Fourier transform infrared spectrometry of ZIF-8, BSA, and BSA@ZIF-8. (d) The zeta-potentials of ZIF-8 and BSA@ZIF-8.

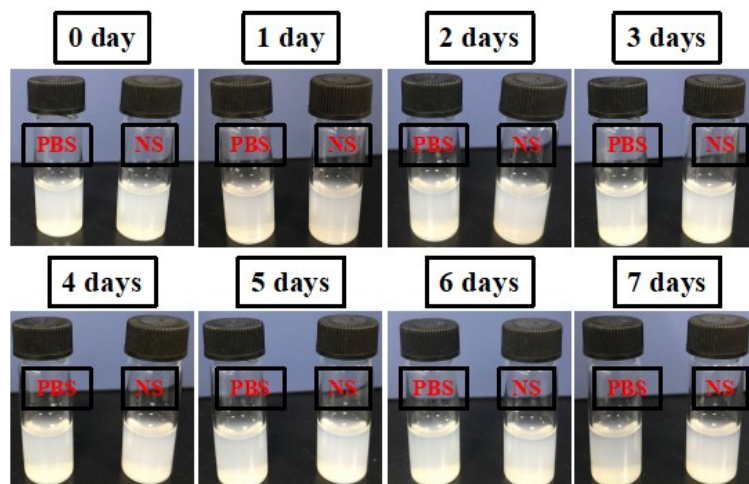


Figure S3. The photographs of BSA@ZIF-8 dispersion in PBS solutions and normal saline for 0 day, 1 day, 2 days, 3 days, 4 days, 5 days, 6 days, and 7 days.

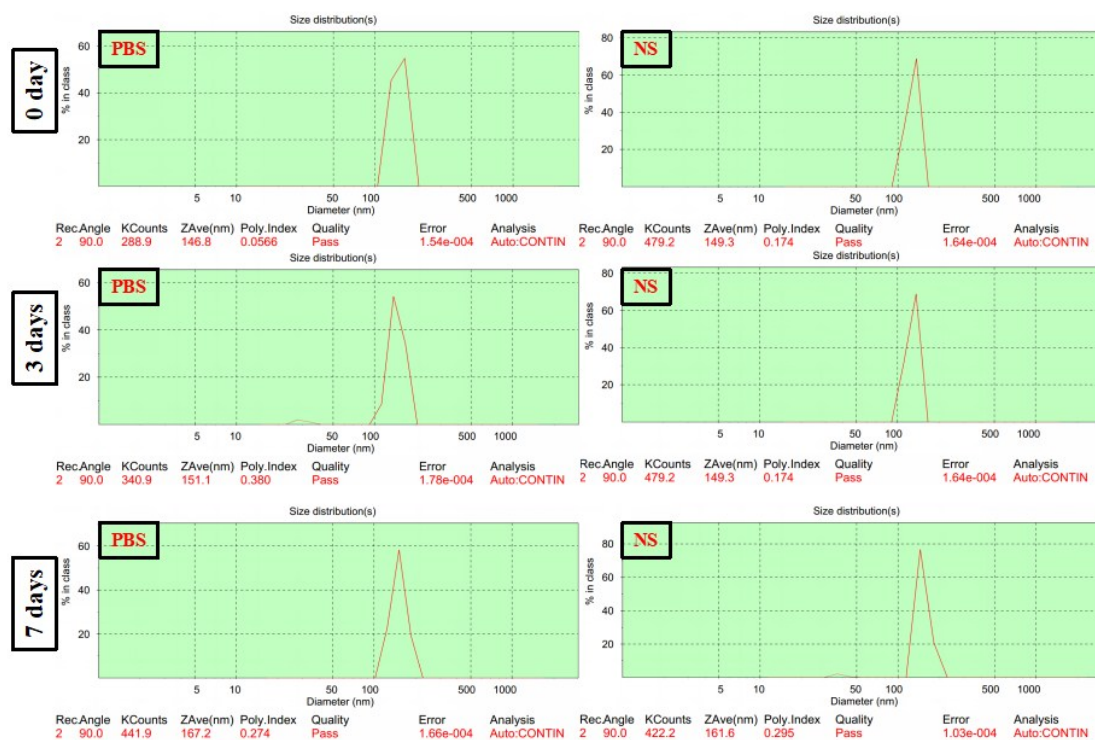


Figure S4. The hydrodynamic diameter of BSA@ZIF-8 in PBS solutions and normal saline for 0 day, 3 days, and 7 days.

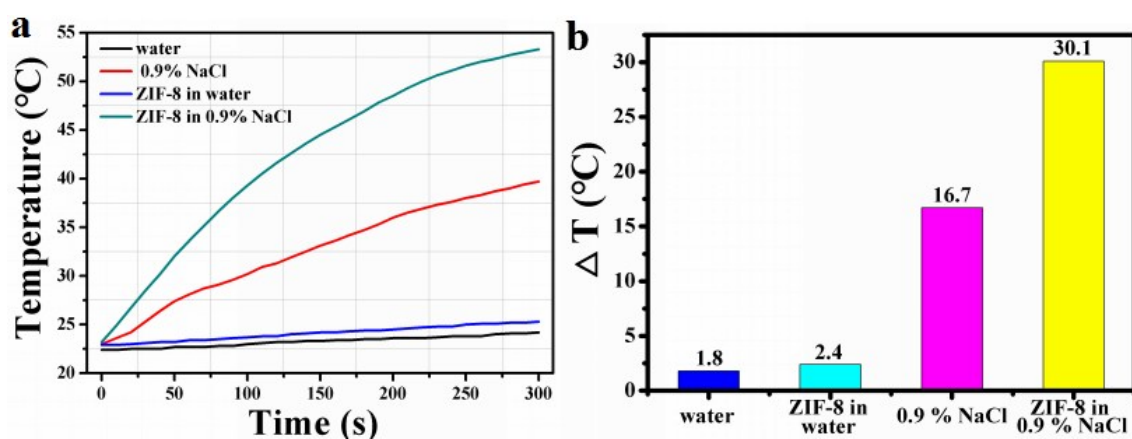


Figure S5. (a) The heating curves of the ZIF-8 in water and saline solution at 10 mg mL⁻¹ under 5 min 1.8 W and 450 MHz microwave irradiation. (b) Temperature change values of different solutions based on (a).

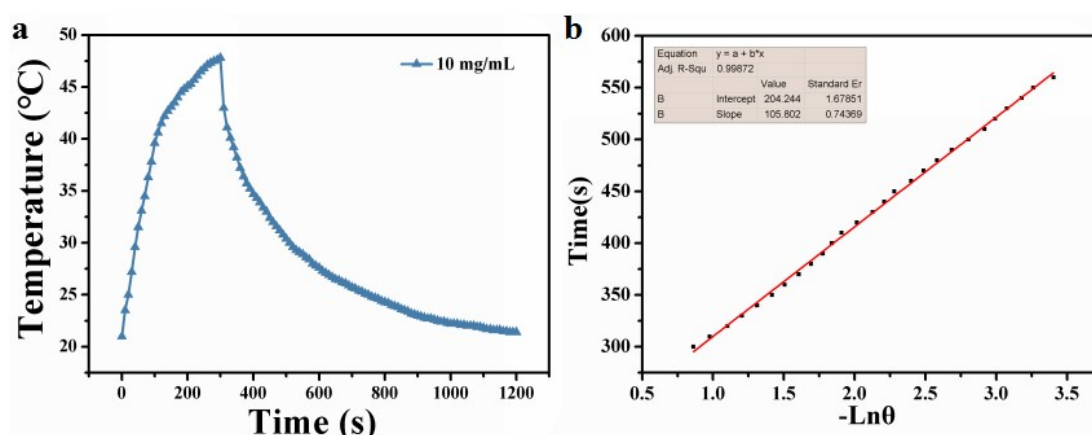


Figure S6. (a) The heating curve of the BSA@ZIF-8 in saline water with 1.8 W microwave irradiation for 5 min at 10 mg mL⁻¹ and then the laser was shut off. (b) Linear time data versus $-\ln\theta$ obtained from the cooling period.

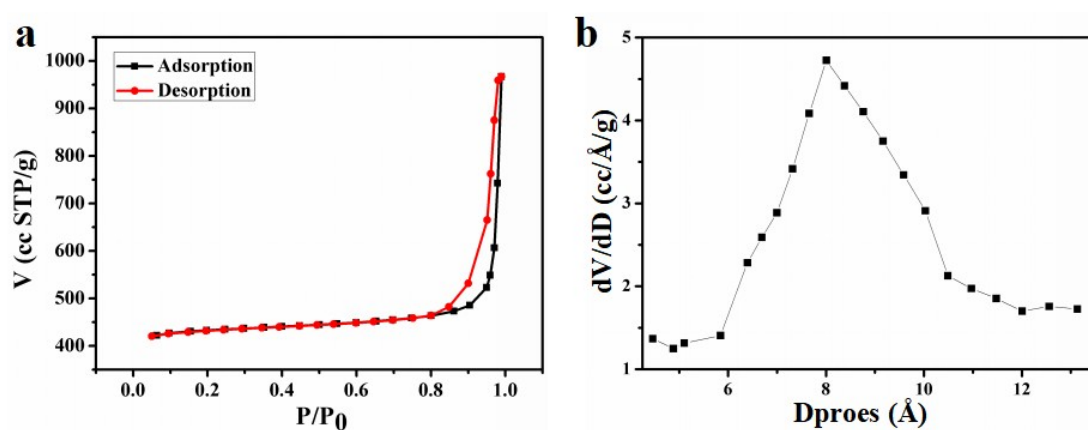


Figure S7. (a) N₂ isothermal adsorption–desorption and (b) micropore size distribution curves of ZIF-8.

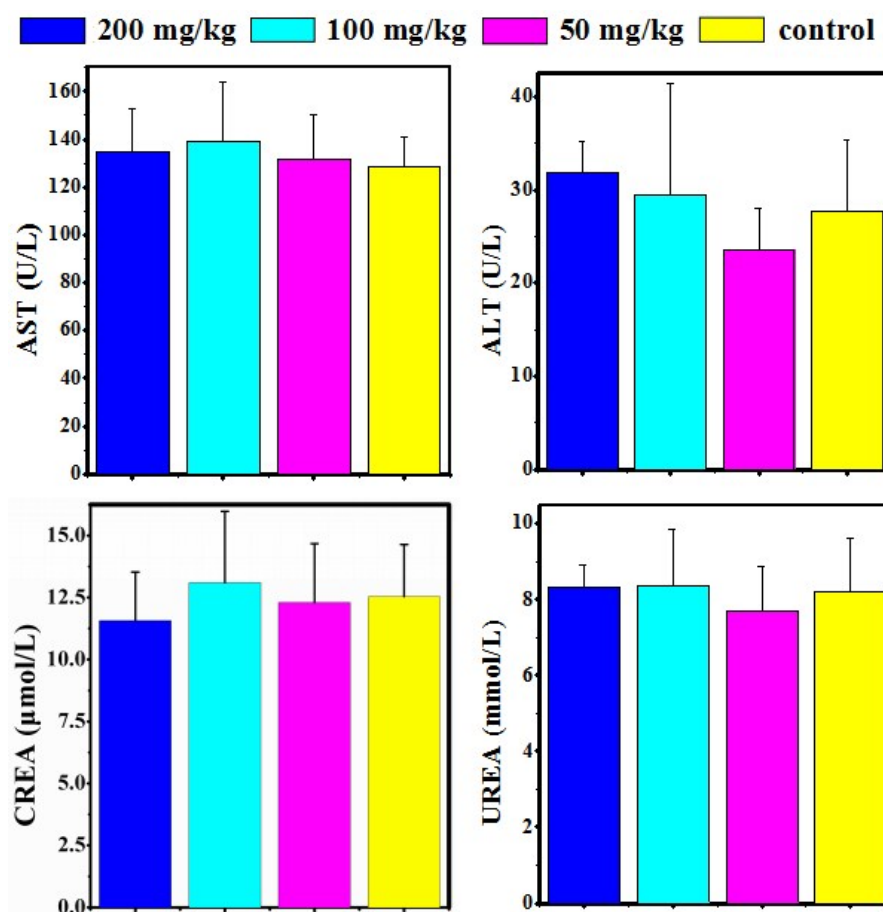


Figure S8. Blood biochemical analysis including AST, ALT, CREA, and UREA of each group for BSA@ZIF-8 (0, 50, 100, and 200 mg kg⁻¹) via tail vein injection in vivo.

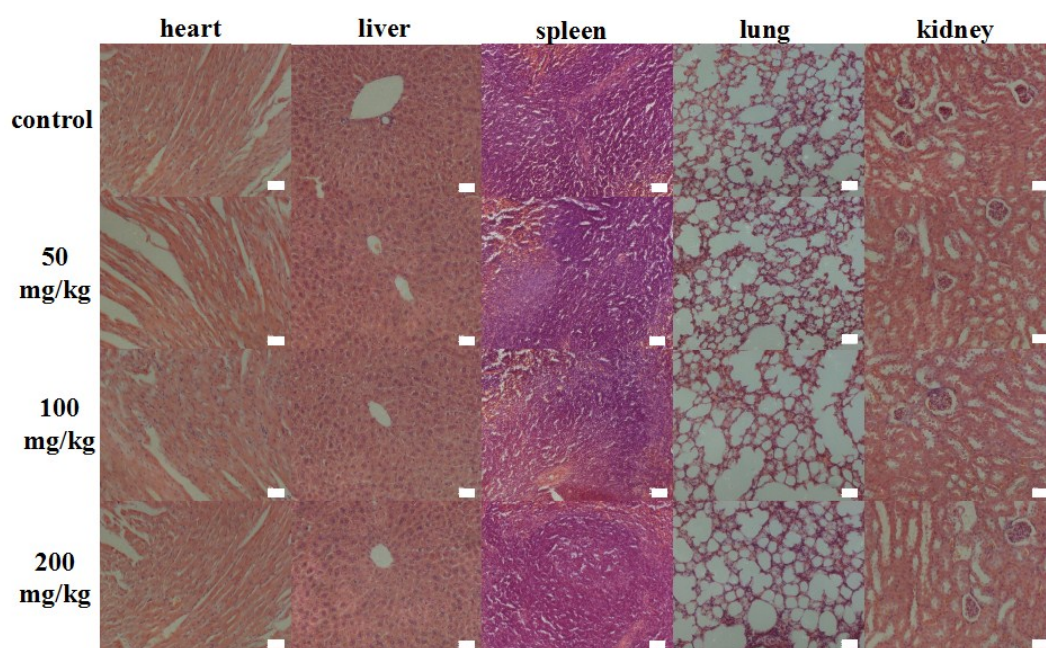


Figure S9. H&E staining images of various organs (heart, liver, spleen, lung, and kidney) of each experimental group (0, 50, 100, 200 mg kg⁻¹). (Scale bar 50 μm for all images).

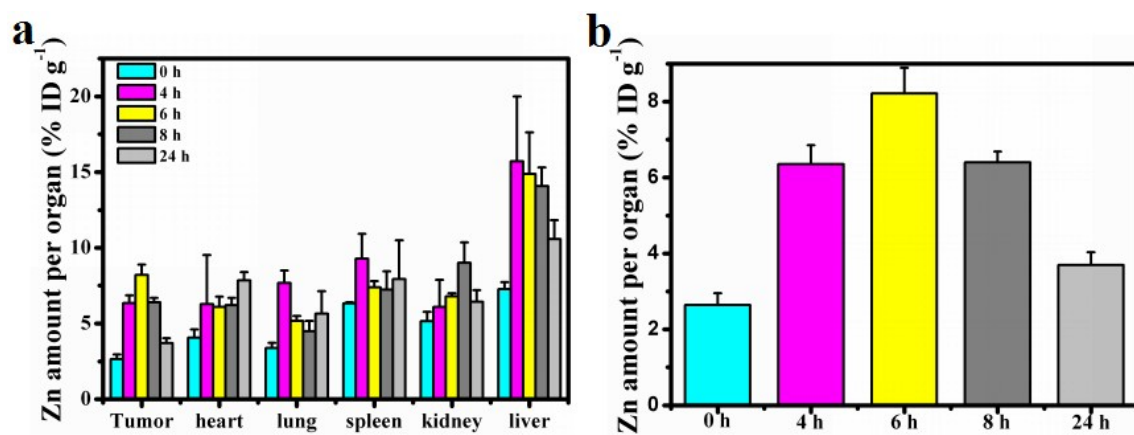


Figure S10. (a) Content of Zn in per organ after intravenous injection of BSA@ZIF-8 (50 mg kg⁻¹) at different times (0, 4, 6, 8, and 24 h). (b) Content of Zn in tumor after intravenous injection of BSA@ZIF-8 (50 mg kg⁻¹) at different times (0, 4, 6, 8, and 24 h).

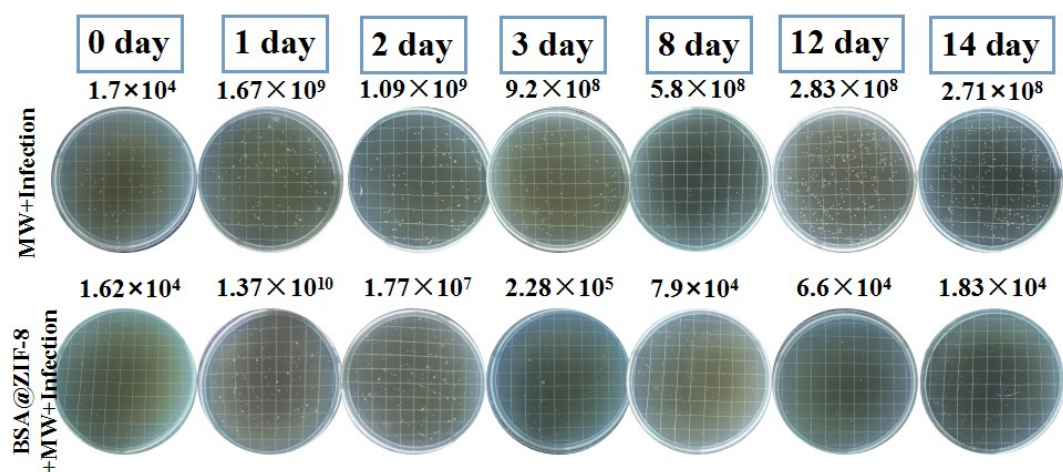


Figure S11. The bacterial colony spread plate photos of MW+infection group and BSA@ZIF-8+MW+infection group for 14 days.

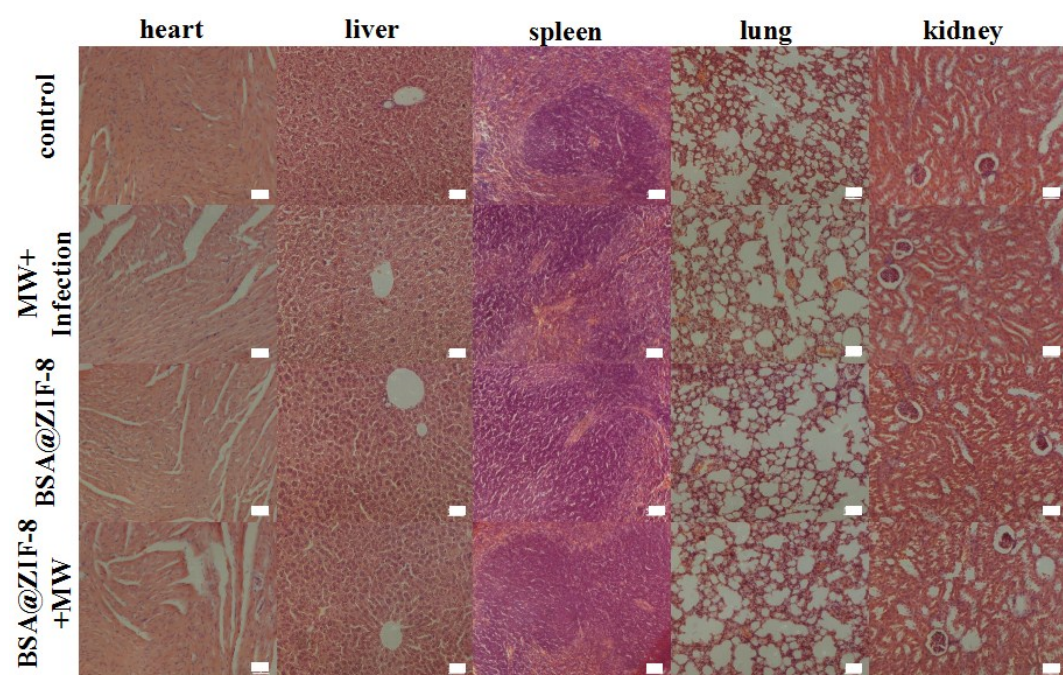


Figure S12. Representative histology H&E staining images of various organs (heart, liver, spleen, lung, and kidney) of different treated groups. (Scale bar 50 μm for all images).

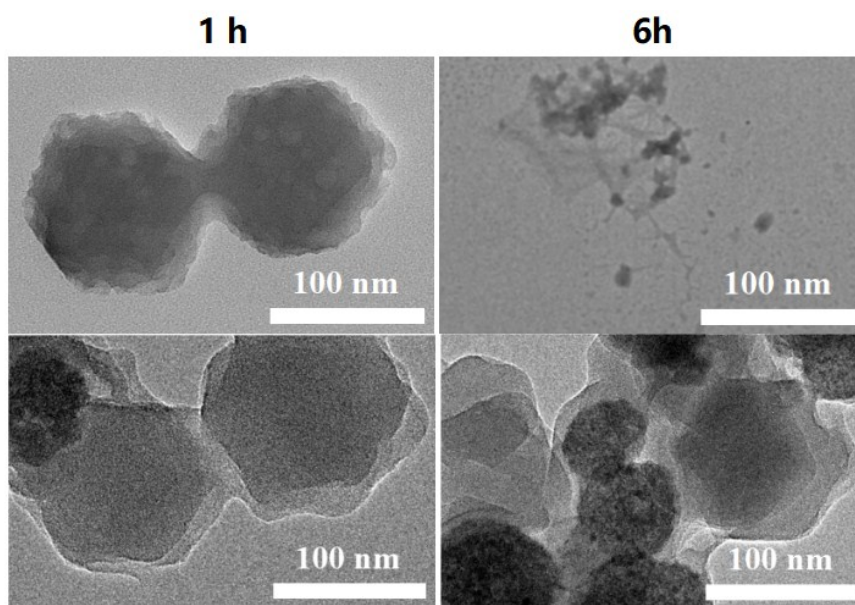


Figure S13. Degradation of ZIF-8 and BSA@ZIF-8 at different time periods in acidic condition (pH 5.5 phosphate-buffered saline) in vitro.

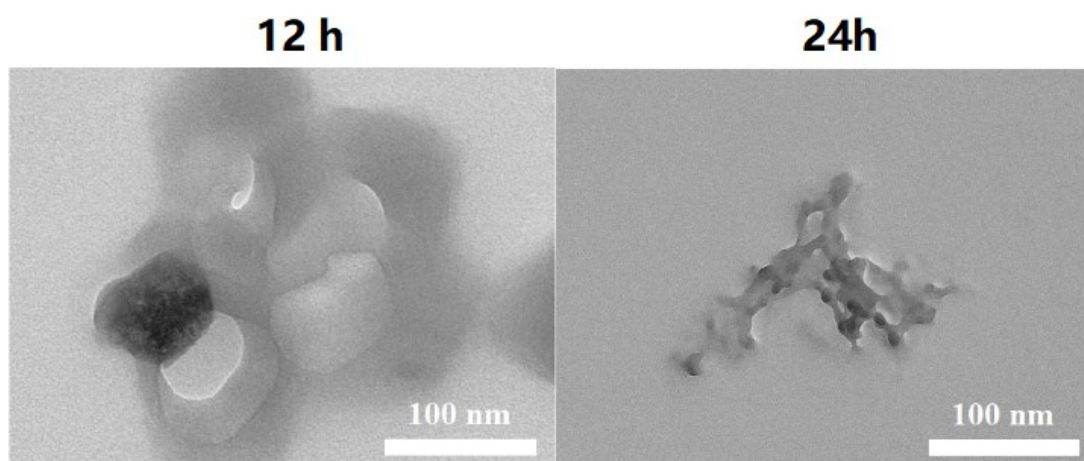


Figure S14. Degradation of BSA@ZIF-8 at different time periods in acidic condition (pH 5.5 phosphate-buffered saline) in vitro.